◆ Human Brain Mapping 29:858–867 (2008) ◆

Resting in Peace or Noise: Scanner Background Noise Suppresses Default-Mode Network

Nadine Gaab,[1,2*] John D.E. Gabrieli,[2] and Gary H. Glover[3]

[1]*Developmental Medicine Center, Children's Hospital Boston, Harvard Medical School, Boston, Massachusetts*
[2]*Department of Brain and Cognitive Sciences, MIT, Cambridge, Massachusetts*
[3]*Department of Radiology, Stanford University, Stanford, California*

Abstract: Studies have identified specific brain regions that increase activation during rest relative to attention-demanding tasks; these regions subserve the "default mode of brain function''. Most of these studies have been conducted in the presence of scanner background noise (SBN). This noise has been shown to lead to altered attentional demands, and thus may modulate the default-mode network. Twelve subjects were examined during a rest condition that was contrasted with an auditory task. Words were presented either with SBN employing a conventional acquisition or without SBN using a sparse sampling approach. The number of experimental and resting trials was equated between the designs. Selecting the images in the condition with SBN that corresponded in time with the images in the condition without SBN made a direct comparison of the default-mode network (rest contrasted with active task) possible. There was typical activation of the default-mode network during rest versus task for both designs. However, SBN suppressed major components of the default-mode network, including medial prefrontal cortex, posterior cingulate, and precuneus. Our results suggest that the default mode of brain function differs when assessed in the presence compared to the absence of scanner noise, with the presence of scanner noise perhaps adding attentional demands that diminish activation changes between rest and task in a nonlinear way within the default network. Further studies are needed to clarify whether the use of a sparse sampling technique might enhance clinical utilities that have been proposed for analysis of the default-mode network. *Hum Brain Mapp 29:858–867, 2008.*

Key words: fMRI; default mode of brain function; scanner background noise; masking

INTRODUCTION

Many studies using functional magnetic resonance imaging (fMRI) or positron emission tomography (PET) have identified a network of brain regions that demonstrate greater activation during a resting period than during engagement in attention-demanding goal-directed tasks. Because this network is ubiquitously more active during rest than during a broad range of tasks, it has been called the default-mode network [Binder et al., 1999; Fox et al., 2005; Greicius and Menon, 2004; Greicius et al., 2003; Gusnard and Raichle, 2001; Mazoyer et al., 2001; McKiernan et al., 2003; Raichle et al., 2001]. Typical regions that show these activations during rest include posterior cingulate cortex, medial prefrontal cortex, anterior parietal regions, ventral anterior cingulate, precuneus, and medial temporal/parahippocampal regions [Greicius et al., 2003; Gusnard and Raichle, 2001; Raichle, 2001].

The default-mode network was discovered in silent PET studies [Raichle et al., 2001], but most current studies

Contract grant sponsor: NIH; Contract grant number: RR09784.

*Correspondence to: Nadine Gaab, PhD, Assistant Professor, Children's Hospital Boston, Harvard Medical School, Developmental Medicine Center, 1 Autumn Street, Room AU611, Boston, MA 02215-5365, USA. E-mail: nadine.gaab@childrens.harvard.edu

Received for publication 28 October 2007; Revised 28 January 2008; Accepted 6 March 2008

DOI: 10.1002/hbm.20578

Published online 2 May 2008 in Wiley InterScience (www.interscience.wiley.com).

assessing activations associated with "rest" or doing "nothing" [Fransson, 2005] employ fMRI, and therefore have been conducted in the presence of scanner background noise (SBN). This noise accompanies every conventional fMRI measurement and can reach noise levels up to 130 dB [for a review see Amaro et al., 2002; Moelker and Pattynama, 2003]. Assessing the default-mode network in the presence of a loud auditory stimulus (SBN) might differ from its assessment during uncontaminated silence. The default-mode network might therefore not represent the true default-mode network but rather the default-mode network in the presence of a loud continuous auditory stimulus.

Studies using PET to detect the default mode of brain region network found similar brain networks when compared to the fMRI studies. However, a direct comparison to assess the influence of SBN is difficult because of the differences in sensitivity and limitations of the PET study duration necessitating differences in overall session lengths and number of presented trials. Furthermore, a comparison of signal intensities between the silent method (PET) and the noisy method (fMRI) cannot be performed because of the differences of the dependent variables (rCBF vs. BOLD signal).

Several studies have shown that SBN can have complex influences on activations. Nonlinear effects in response to SBN have been reported, suggesting that SBN in the experimental and control conditions is not "canceling" out when conditions are contrasted against each other [Gaab et al., 2007a,b; Talavage and Edmister, 2004]. Therefore, the effects of SBN on activation within cortical areas can differ between the experimental and control condition. Additionally, it has been suggested that increased attentional or cognitive resources are invoked in studies with continuous SBN compared to studies with less SBN [Gaab et al., 2007a,b; Tomasi et al., 2005]. Listening to words in the presence of SBN seems more like a selective or divided attention task where attention to one set of stimuli (e.g. words) is required, whereas cognitive inhibition is necessary to neglect the second set (SBN).

Therefore, one could hypothesize that SBN as a source of external stimulation could suppress activation of the default-mode network, defined as the resting state in contrast to an active task. If so, employment of a silent scanning design such as sparse temporal sampling [e.g., Belin et al., 1999; Gaab et al., 2003; Hall et al., 2000] would reveal increased activation of the default-mode network. We examined our hypothesis regarding the influence of SBN by varying the degree of SBN during a silent rest interval, which was contrasted with an active auditory task, but keeping the number of acquisitions and experimental stimulation constant. If the SBN adds an additional cognitive or attentional demand to the brain, it will augment the task-induced metabolic demand in some fashion. Because other studies have shown that the influence of SBN is nonlinear in auditory regions, it is reasonable to suppose that the influence of SBN will be nonlinear in the default mode network as well. Therefore, one would expect altered activation of the default mode network (i.e., resting − task contrast) with SBN present compared to scans without SBN. The most likely form of nonlinearity is a saturation of the default mode activation as total metabolic demand increases, in which case the influence of SBN would be to decrease the observed default mode network activation. However, if the default mode network activation is linear with total task demand (including SBN) then the SBN will have equal and noninteractive influences on both rest and task conditions, in which case activation of the default-mode network (rest − task contrast) would be equal with or without SBN.

METHODS

Participants

Twelve healthy right-handed volunteers (mean age: 21.3) participated in this study. Informed consent was obtained from each subject in accordance with a protocol approved by the Stanford IRB.

Imaging Procedure

The fMRI scanning was conducted with a 3.0 T GE Signa scanner (General Electric, Milwaukee, WI). T1-weighted whole-brain anatomy scans were collected and high order shimming was employed [Kim et al., 2002]. The fMRI data were collected using a spiral in/out T2* pulse sequence [Glover and Law, 2001] (30 slices, 64 × 64 voxels, 3.43 mm inplane resolution, TE 30 ms, 4 mm slice thickness, 0.5 mm skip).

Two types of acquisitions were used, a conventional continuous acquisition that included SBN throughout the rest intervals and a sparse sampling acquisition [STsamp; Gaab et al., 2003, 2007a,b] that measured responses following periods of silent intervals. The slice prescription for the two experimental conditions was kept constant as was the approximate duration of the scans. During the SBN- acquisition, the 30 slices were acquired in the first 1.995 s of the 16 s TR period. Therefore, images were only acquired every 16 s and no SBN was present for ~14 s following the ~2 s acquisition time. In the continuous scan condition, the 30 slices were spaced evenly throughout the 2 s TR, which resulted in continuous SBN throughout the experiment.

Stimuli and Experimental Tasks

All subjects underwent two experimental scan runs of differing acquisition type and were instructed to perform the same task in both scans (see Fig. 1]. During the active condition, they listened to a series of four words and had to decide whether two of the four presented words were the same or not. This experimental condition was contrasted with a rest control condition [details in Gaab et al., 2007a,b]. No specific instruction was given for the rest conditions. Because of the nature of the experimental

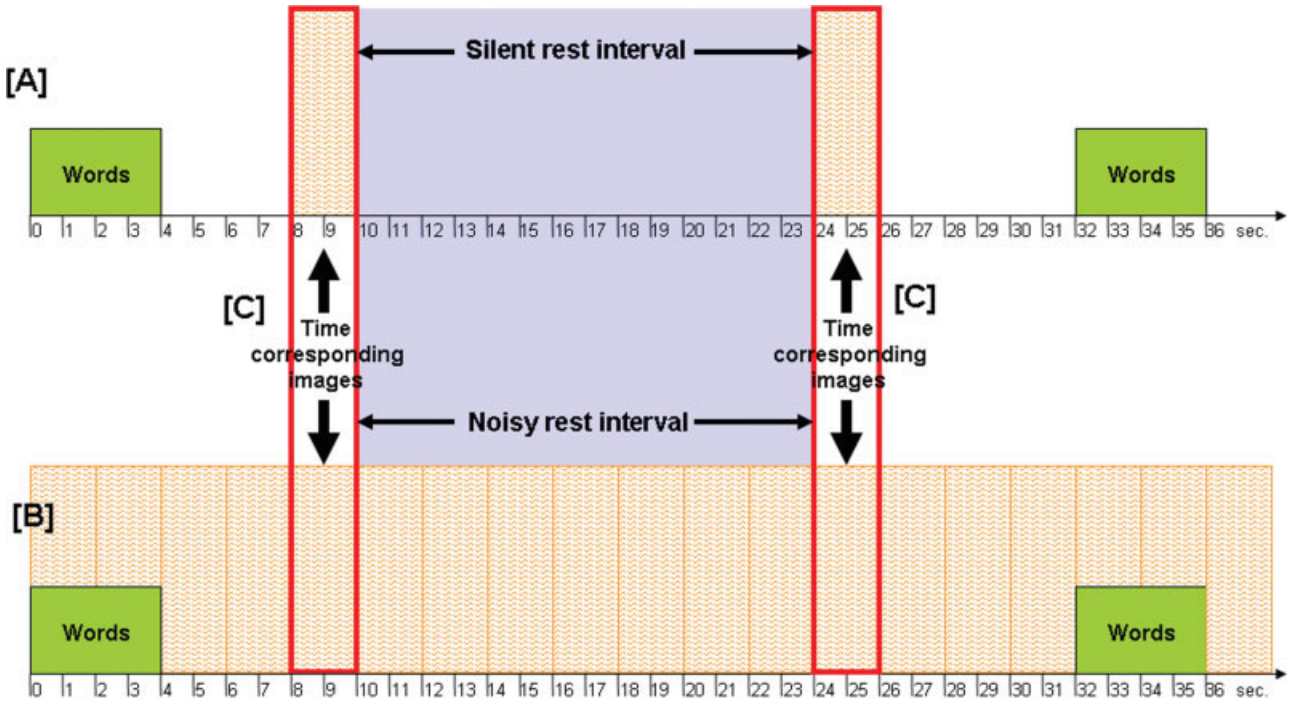

Figure 1.

Experimental design. [**A**] represents the sparse temporal sampling technique with reduced SBN during the active condition and silent rest intervals; [**B**] represents the design with continuous SBN and noisy rest intervals. Orange shaded boxes indicate scan acquisitions, while the green boxes represent the auditory stimulation (four words). The auditory stimulation was identical between the two designs and 64 images were selected out of all images acquired during ERcont (B) that corresponded in time to the images acquired during STsamp (A). These images are represented by the red boxes [**C**].

design (see below), subjects could not anticipate rest conditions.

Sparse temporal sampling design (STsamp)

Subjects listened to 48 sets of words and 16 silent periods with the TR held constant at 16 s (flip angle 90°). The start of the 2 s clustered MR acquisition varied with regard to the onset of auditory stimulation by pseudo-randomly jittering the start of the auditory stimulation frame within the 16 s TR period [Fig. 1A; for details see Gaab et al., 2003]. Overall, 64 time frames were acquired (17 min/34 s).

Event-related continuous scanning design (ERcont)

The ERcont condition involved the same auditory stimulation design as the STsamp task, but with the continuous scanner noise during the entire experiment as occurs typically in event-related fMRI experiments (Fig. 1B). A TR of 2 s was used for this condition with flip angle 75° (17 min/12 s; 516 time frames).

Selecting time-correspondent scans (ER64)

To directly test the influence of the SBN on the default-mode network without interference of the number of images acquired, we selected 64 evenly spaced images out of the 516 images in the ERcont condition. The selected scans (ER64; Fig. 1C), here named "matched" scans, corresponded exactly in time with the 64 images in the STsamp condition. The order of the three designs was pseudo-randomized between subjects.

fMRI Data Analysis

fMRI data preprocessing

After image reconstruction, each set of axial images was slice time corrected, realigned to the first image and co-registered with the corresponding T1-weighted high-resolution data set, spatially normalized and smoothed with a 4 mm isotropic Gaussian kernel. Grand mean scaling was not performed.

Statistical analysis of group fMRI data

The main statistical data analysis was performed using a general linear model as implemented in SPM2 [Friston et al., 1995; Wellcome Department of Cognitive Neurology, London, UK]. Statistical thresholds were varied because of differences in statistical power for the various analyses.

Main effects within each experimental design

By convolving the silent (STsamp) and noisy (ER64) 14 s rest intervals with a hemodynamic response function (HRF) [Glover, 1999] a covariate "default" was developed and utilized as a regressor in two separate (ER64 and STsamp) simple regression analyses. This technique treats the rest intervals (silent for STsamp and noisy for ER64) as a 14 s event, which starts right after the end of scan X and lasts 14 s until the beginning of scan $X + 1$. Furthermore, the same technique was chosen for the active task. However, only the 4 s of the auditory stimulation were treated as an event excluding the no-stimulation periods prior and after the auditory stimulation within one TR. The contrast images so obtained for each subject were then entered into an overall random-effects group analysis (for both experimental designs combined) and two separate random-effects one sample t-tests (one for each experimental design). The combined analysis was analyzed using a threshold of $P < 0.001$ (extent: 50; uncorrected for multiple comparisons). This was chosen in order to obtain relatively large clusters for the ROI analysis. A less conservative threshold was used for each design separately ($P < 0.005$, extent: 25; uncorrected for multiple comparisons), since statistical power is lower in the separate analyses when compared to the combined analysis.

Between design effects

To compare the STsamp and the ER64 design, we performed a paired t-test (random-effects analysis) with the contrast images (silent rest interval or noisy rest interval contrasted versus all other images). If the SBN has no influence on the default-mode network then these two designs should be identical and a paired t-test should reveal no difference. For this between design analysis a threshold of $P < 0.005$ (extent: 15; uncorrected for multiple comparisons) was chosen to reveal smaller clusters as well.

ROI delineation

The overall group analysis (both experimental designs combined) was used in order to obtain functionally defined "regions of interest" (ROIs). Our analysis revealed 12 ROIs (Tables I and V). Two individual contrast maps (silent rest interval or noisy rest interval contrasted versus all other images) were created for each subject (STsamp and ER64) using a single regression analysis with the corresponding covariates (see above) and region-specific values were averaged for each of the two experimental designs. Furthermore, the ROIs were applied to the active word task and weighted parameter estimates were obtained. For the active task, a covariate "active" was developed by convolving the task with a HRF [Glover, 1999] [see Gaab et al., 2007a,b for more details].

TABLE I. Activation table for the combined default-mode network analyses of ER64 and STsamp

Region	Extent	MNI coordinates			T
		x	y	z	
Left middle temporal gyrus	855	−42	−74	22	6.78
Left angular gyrus		−48	−72	30	6.62
Middle temporal gyrus		−48	−64	16	5.69
Right middle temporal gyrus	853	44	−60	18	8.10
Right anterior cingulated		50	−72	30	6.25
Right middle occipital gyrus		36	−80	20	5.64
Right precuneus	255	18	−60	24	5.85
Right posterior cingulated		12	−48	18	5.14
Left middle frontal gyrus	235	−22	18	46	5.79
Middle frontal gyrus		−22	26	40	5.62
Left superior frontal gyrus		−32	30	48	5.13
Left posterior cingulated	209	−10	−50	22	4.81
Left precuneus		−14	−50	30	4.47
Medial frontal gyrus	149	2	48	−8	4.67
Medial frontal gyrus		10	54	0	4.41
Left anterior cingulated		−2	40	−6	4.46
Left superior frontal gyrus	144	−8	56	34	6.54
Left superior frontal gyrus		−18	42	34	4.51
Left superior frontal gyrus		−20	38	42	4.40
Left precuneus	143	−24	−84	40	6.08
Left cuneus		−24	−82	30	4.57
Right precuneus	114	12	−60	64	4.97
Right precuneus		16	−56	58	4.01
Left parahippocampal gyrus	98	−30	−38	−2	5.09
Left parahippocampal gyrus		−20	−42	4	5.07
Right paracentral lobule	83	10	−30	52	5.79
Right cingulate gyrus		14	−28	40	3.98
Right middle frontal gyrus	73	28	28	44	5.13
Right middle frontal gyrus		28	14	44	4.15

Extent is presented in voxel. MNI, montreal neurological institute. T is presented in t-values. Data presented for $P < 0.001$, uncorrected (Cluster size ≥ 50). The top row of each cluster (indicated by numbers) shows the center peaks for the ROIs (see also Table V).

IMAGING RESULTS

For our purpose, we will define positive weighted parameter estimates when assessed with the covariates "default" as "activation" of the default-mode network. Negative parameter estimates when assessed with the covariate "default" will be defined as "deactivation" of the default-mode network. Furthermore, positive weighted parameter estimates when assessed with the covariate "active" will be defined as activation for the active word task and negative parameter estimates will be defined as deactivation for the active word task.

Within Design Analyses

For the combined analyses of ER64 and STsamp, there was activation of the default-mode network regions typically activated during rest contrasted with all other images, including medial frontal gyrus, anterior cingulate, and posterior cingulate (Table I; Fig. 2). Activations in

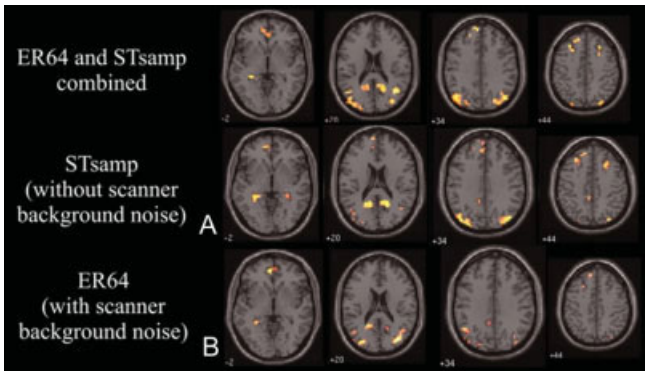

Figure 2.

First row: The default-mode network for STsamp and ER64 combined. Data presented for $P < 0.001$, uncorrected (Cluster size ≥ 50). Second row: The default-mode network for STsamp. Data presented for $P < 0.005$, uncorrected (cluster size = 25). Third row: The default-mode network for ER64. Data presented for $P < 0.005$, uncorrected (cluster size = 25).

most of these regions were also evident in separate analyses of the STsamp (Table II) and ER64 (Table III) conditions (see Fig. 2).

Between Design Analyses

Direct comparison of the two designs revealed significantly greater activation during rest contrasted with all other images for scanning without SBN than with SBN in anterior cingulate, medial temporal/parahippocampal regions, bilateral precuneus, and inferior parietal regions (see Fig. 3) and Table IV.

ROI analysis for default-mode network (Table V, parts a and b; Fig. 4; all statistical tests were uncorrected for multiple comparisons): Parameter estimates for each subject were compared between the STsamp and ER64 in each of the 12 ROIs that had the greatest activation during rest for the combined conditions (Table I). Increased weighted parameter estimates for scanning without SBN vs. scanning with SBN were found for the posterior cingulate, the bilateral precuneus, medial frontal gyrus, and other regions.

Examination of the weighted parameter estimates provides information about why default-mode network activations were greater without SBN than with SBN, specifically whether the activation differences arose from increased deactivations of the default-mode network during the active task condition, increased activation of the default network during the rest condition, or both (see Fig. 4). If the SBN has an influence on the active task by adding additional cognitive load to the verbal working memory task, then one would expect greater deactivations of the default-mode network during the active task. Ten of the 12 ROIs showed significantly greater activation during rest without SBN than with SBN, including posterior cingulate, left and right precuneus, and medial frontal gyrus. Only three ROIs showed significantly decreased activation (or deactivation) during the active condition, posterior cingulate, medial frontal gyrus, and right paracentral lobule. Thus, SBN had a consistent influence on activation during rest, and this was most likely enhanced by an additional influence during the active task in the posterior cingulate and the medial frontal gyrus.

DISCUSSION

We examined the influence of SBN on the default-mode network by varying the degree of SBN across two designs in an event-related verbal working memory fMRI design and resting baseline, while keeping the number of acquisitions and experimental stimulation constant. SBN suppressed major components of the default-mode network, including medial prefrontal cortex, posterior cingulate, and precuneus. In medial prefrontal cortex and posterior cingulate, listening to SBN while performing an active verbal working task led to decreased activations of the default-mode network most likely due to the increased cognitive

TABLE II. Activation table for default-mode network analyses of STsamp

Region	Extent	MNI coordinates			
		x	*y*	*z*	*T*
Left precuneus	628	−42	−70	32	6.98
Left superior occipital gyrus		−40	−84	30	6.30
Left superior frontal gyrus	459	−28	30	48	8.95
Left superior frontal gyrus		−20	28	54	6.71
Left middle frontal gyrus		−24	−38	−4	6.29
Right superior occipital lobe	445	40	−82	22	6.58
Right angular gyrus		46	−74	32	6.58
Right precuneus		32	−80	44	6.12
Left posterior cingulate/precuneus	284	−12	−56	22	5.35
Left posterior cingulate		−20	−52	14	4.22
Right posterior cingulate	256	20	−58	22	7.20
Left medial frontal gyrus	225	−4	40	34	5.19
Left superior frontal gyrus		−14	58	28	4.47
Left medial frontal gyrus		−12	60	16	4.44
Left hippocampus	184	−26	−38	−4	7.35
Left parahippocampal gyurs		−20	−48	2	4.60
Left anterior cingulate	136	−14	40	−4	6.04
Left anterior cingulate		−8	50	2	5.31
Right superior parietal gyrus	122	18	−54	60	3.62
Right precuneus		8	−52	56	3.50
Right middle frontal gyrus	67	26	22	44	4.70
Right middle frontal gyrus		28	14	44	4.34
Right parahippocampal gyrus	62	34	−42	0	6.71
Right parahippocampal Gyrus		26	−36	−6	3.84
Right Middle Temporal Gyrus		44	−56	12	3.89
Right Middle Temporal Gyrus		42	−58	4	3.84
Left Precuneus	34	−4	−38	46	6.28
Left Cingulate Gyrus		−10	−44	40	4.21

Extent is presented in voxel. MNI, montreal neurological institute. *T* is presented in *t*-values. Data presented for $P < 0.005$, uncorrected (cluster size = 25).

TABLE III. Activation table for default-mode network analyses of ER64

Region	Extent	MNI coordinates			T
		x	y	z	
Right middle temporal gyrus	619	46	−58	8	5.95
Right angular gyrus		38	−78	32	5.48
Left angular gyrus	546	−28	−82	22	10.09
Left middle temporal gyrus		−52	−72	30	5.30
Right precuneus/cingulate gyrus	125	16	−50	26	7.41
Right posterior cingulate		12	−50	16	4.46
Left parahippocampal gyrus	91	−28	−44	0	5.72
Left parahippocampal gyrus		−36	−42	−6	3.83
Left cingulate/posterior cingulate	79	−22	−52	24	7.13
Left medial frontal gyrus	73	−8	48	−6	6.96
Medial frontal gyrus		6	50	−4	3.81
Left precuneus/cingulate gyrus	40	−8	−48	36	4.38
Left superior frontal gyrus	30	−10	42	44	4.15
Right insula	29	36	−4	16	3.94
Left middle frontal gyrus	28	−24	22	44	3.81
Left superior frontal gyrus		−28	26	50	3.33
Right postcentral gyrus	27	6	−50	66	6.24

Extent is presented in voxel. MNI, montreal neurological institute. T is presented in t-values. Data presented for $P < 0.005$, uncorrected (cluster size = 25).

load resulting from the addition of SBN to task performance.

Typical regions of the default mode of brain function were observed in designs with and without SBN, including posterior cingulate, bilateral precuneus, anterior cingulate, medial frontal gyrus, and left parahippocampal gyrus. Thus, SBN does not alter spatial characteristics of the default-mode network, but instead influences the magnitude of activations in that network. The SBN-induced change in default-mode network activation indicates that

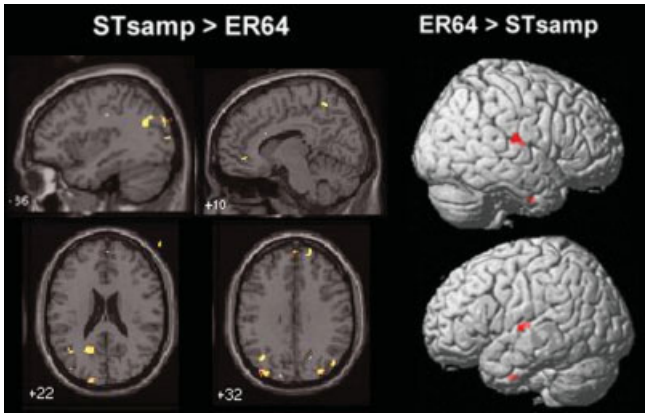

Figure 3.
Statistical comparison (paired t-test) for the default-mode network between ER64 and STsamp. Data presented for $P < 0.005$, uncorrected (cluster size = 15.

TABLE IV. Activation table for default-mode network between design analyses for STsamp > ER64 and ER64> STsamp.

Region	Extent	MNI coordinates			T
		x	y	z	
ER64 > STsamp					
Right insula	29	44	−18	16	6.35
Right superior temporal gyrus		42	−12	10	3.40
Left superior temporal gyrus	19	−46	−10	4	4.08
Left Insula		−40	−18	6	3.30
STsamp> ER64					
Left middle temporal gyrus	72	−48	−66	16	4.90
Left middle temporal gyrus		−38	−62	16	4.20
Right cuneus	59	32	−84	34	5.03
Right cuneus		34	−76	40	3.31
Left precueus	45	−14	−70	36	5.88
Left precuneus		−8	−72	44	3.60
Right angular gyrus	44	46	−74	32	5.92
Right postcentral gyrus/inferior parietal gyrus	42	30	−28	42	5.93
Right middle temporal gyrus	38	44	−58	4	5.19
Right middle occipital gyrus		38	−66	0	3.88
Right precuneus	32	16	−68	36	5.54
Right precuneus		18	−64	44	5.16
Right precuneus		8	−72	36	4.20
Right anterior cingulate	31	12	42	−4	4.76
Right anterior cingulate		20	40	−6	3.94
Right middle frontal gyrus	28	22	−8	46	6.29
Left cuneus	28	−14	−90	28	4.30
Left cuneus		−16	−94	18	4.14
Superior frontal gyrus	27	0	58	28	7.22
Left parahippocampal gyrus	25	−24	−38	−4	6.26
Left paracentral lobule	23	−12	−38	54	3.93
Left inferior parietal gyrus	21	−36	−30	38	4.42
Left postcentral gyrus		−28	−26	44	3.96
Left precuneus	18	−34	−66	32	4.76
Left superior occipital gyrus	17	−40	−82	32	4.06
Right superior frontal gyrus	15	20	60	32	5.91

Extent is presented in voxel. MNI, montreal neurological institute. T is presented in t-values. Data presented for $P < 0.005$, uncorrected (cluster size = 15).

SBN does not simply add a constant influence that is eliminated when active and rest conditions are contrasted. Rather, SBN interacts with the two conditions nonlinearly.

The default-mode network activation is typically defined by the difference between activity during rest and activity during task performance. Thus, altered default mode of brain function activation with SBN could reflect the influence of SBN on activity level during rest or deactivation during task performance, or both. The ROI analysis revealed that SBN suppressed activation during rest compared to all other nonrest images in most components of the default-mode network, including medial prefrontal cortex, posterior cingulate, and bilateral precuneus. This finding suggests that passive processing of SBN provided enough external stimulation to diminish introspective processes thought to be mediated by the default-mode network [Gusnard et al., 2001; Gusnard, 2005; Fox et al., 2005;

TABLE V. ROI results for (a) default-mode network and (see also Fig. 4).

ROI center	No. of voxel	Anatomy	Result	*P*-value
(a)				
$x = -8/y = 56/z = 34$	144	Left superior frontal gyrus	Not significant	0.480
$x = -10/y = -50/z = 22$	209	Left posterior cingulated	ER64 < STsamp	0.028
$x = -22/y = 18/z = 46$	235	Left middle frontal gyrus	Not significant	0.388
$x = -24/y = -84/z = 40$	143	Left precuneus	Trend: ER64 < STsamp	0.099
$x = -30/y = -38/z = -2$	98	Left parahippocampal gyrus	Trend: ER64 < STsamp	0.071
$x = -42/y = -74/z = 22$	855	Left middle temporal gyrus	ER64 < STsamp	0.002
$x = 2/y = 48/z = -8$	149	Medial frontal gyrus	ER64 < STsamp	0.028
$x = 10/y = -30/z = 52$	83	Right paracentral lobule	Trend: ER64 < STsamp	0.099
$x = 12/y = -60/z = 64$	114	Right precuneus	ER64 < STsamp	0.034
$x = 18/y = -60/z = 24$	255	Right precuneus	Trend: ER64 < STsamp	0.071
$x = 28/y = 28/z = 44$	73	Right middle frontal gyrus	ER64 < STsamp	0.019
$x = 44/y = -60/z = 18$	853	Right middle temp. gyrus	ER64 < STsamp	0.005
(b)				
$x = -8/y = 56/z = 34$	144	Left superior frontal gyrus	Not significant	0.814
$x = -10/y = -50/z = 22$	209	Left posterior cingulate	Trend: ER64 > STsamp	0.099
$x = -22/y = 18/z = 46$	235	Left middle frontal gyrus	Not significant	0.239
$x = -24/y = -84/z = 40$	143	Left precuneus	Not significant	0.480
$x = -30/y = -38/z = -2$	98	Left parahippocampal gyrus	Not significant	0.347
$x = -42/y = -74/z = 22$	855	Left middle temporal gyrus	Not significant	0.182
$x = 2/y = 48/z = -8$	149	Medial frontal gyrus	ER64 > STsamp	0.000
$x = 10/y = -30/z = 52$	83	Right paracentral lobule	ER64 > STsamp	0.002
$x = 12/y = -60/z = 64$	114	Right precuneus	Not significant	0.158
$x = 18/y = -60/z = 24$	255	Right precuneus	Not significant	0.136
$x = 28/y = 28/z = 44$	73	Right middle frontal gyrus	Not significant	0.583
$x = 44/y = -60/z = 18$	853	Right middle temp. gyrus	Not significant	0.239

Fransson, 2005]. In a few regions, including medial prefrontal cortex and posterior cingulate, SBN also led to decreased activation (deactivation) during task performance. This deactivation of default mode of brain function regions can be interpreted as a consequence of the greater perceptual difficulty, attentional demands, or cognitive load in listening to words with SBN present.

Prior studies have found that the magnitude of task-induced deactivations tends to increase with task demands [Daselaar et al., 2004; McKiernan et al., 2003; Tomasi et al., 2005]. The increased attentional demand of SBN (i.e., the greater demand on attention to external stimuli) can explain the significantly higher deactivation in the design with SBN.

Suppression of default-mode network activity during rest (versus all other images) was found in most components of the default-mode network, and may involve a different mechanism. In this case, SBN may provide auditory stimulation that draws attention to the external environment, rather than to introspection of thoughts and feelings. However, this interpretation is challenged by at least two studies. Greicius and Menon [2004] reported that passive visual and auditory stimulation did not lead to modulation of the default-mode network, and listening to SBN can be considered as passive stimulation. Furthermore, using a correlational analysis, Fox et al. [2005] showed high reproducibility of the default-mode network across three different resting states (eyes open, eyes closed, and fixation) for predefined seed regions (posterior cingulate/precuneus, lateral parietal cortex, and medial prefrontal regions), and therefore suggest that default-mode network activation cannot be attributed to the imposition of a low-level tasks. However, both studies employed continuous SBN, which was present throughout all conditions (passive stimulation and rest as well as fixation, eye movements or the presence or absence of visual input) and therefore may have altered all of them. This could have resulted in similar activation of the default-mode network throughout each of the experiments and differences may therefore not be detectable.

Our results suggest that a loud continuous noise (SBN) can suppress the default-mode network activation. The finding that SBN influences active and rest conditions to different degrees suggests a nonlinear influence of the SBN on the default mode of brain function network analogous to that shown for the auditory system before [Gaab et al., 2007a,b; Talavage and Edmister, 2004]. Deactivation in the default mode of brain function regions may exhibit a saturation effect as the total metabolic load due to task activation and SBN increases (see Fig. 5). In this way, as total metabolic load in the brain increases, the deactivation will show a disproportionate increase, and, as suggested in the figure, the net deactivation from task activation will be less when SBN is present. This model is in accordance with our observations.

There is at least one alternative explanation of these results. Our analysis aimed to calculate [rest during silence − words presented during silence] − [rest during SBN − words presented during SBN], which can be rewritten as [rest during silence − rest during SBN] − [words pre-

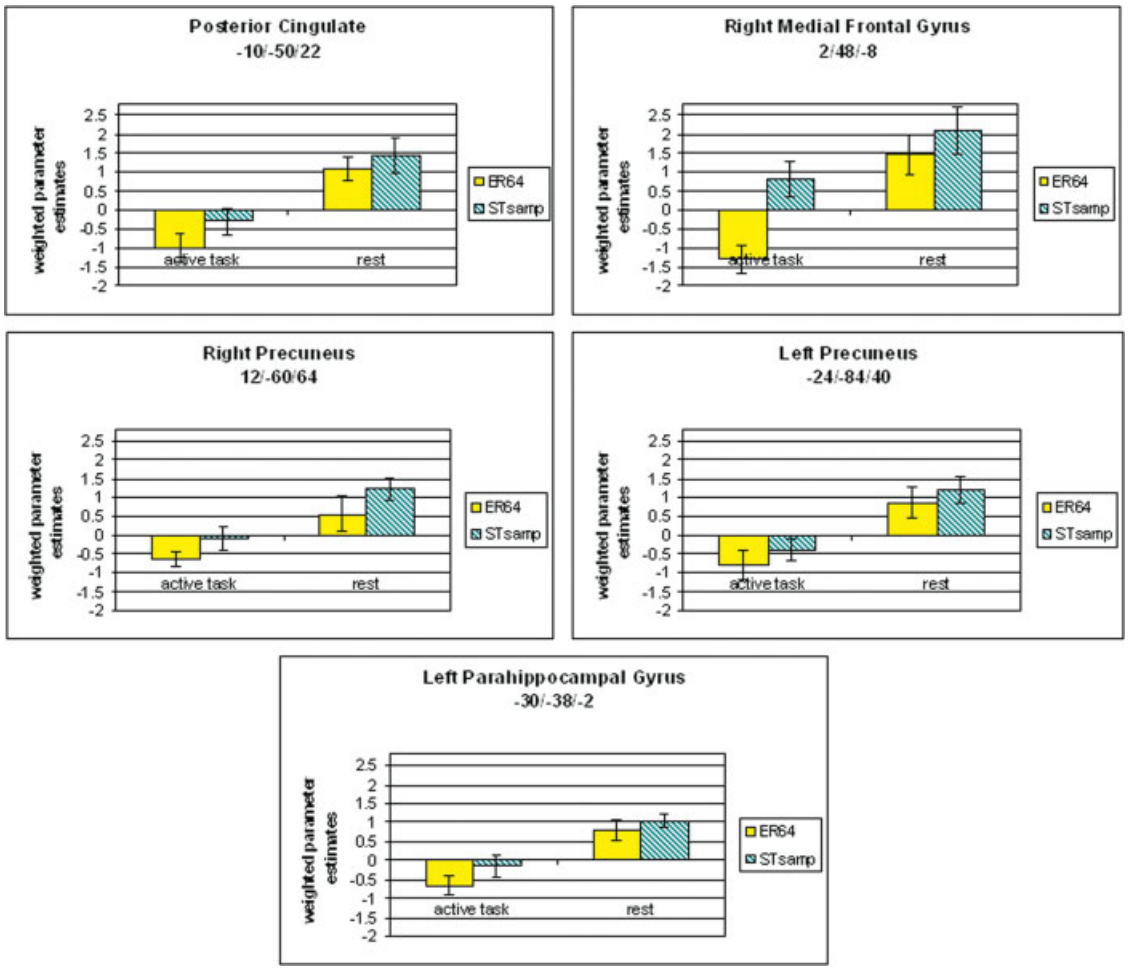

Figure 4.

Yellow/Solid bars: ROI analysis for ER64. Blue/White/striped bars: ROI analysis for STsamp. The ROIs were derived from the combined default-mode network analysis (see Fig. 2, first row). Weighted parameter estimates for the active task are plotted on the left side of each graph. Values for the rest condition are plotted on the right side (**$P < 0.05$; *$P < 0.1$).

sented during silence − words presented during SBN]. Our analysis assumes that the second term [words presented during silence − words presented during SBN] equals null and that the active task can be used as a common baseline across the two conditions. However, most studies investigating the influence of SBN show an influence of SBN on auditory regions [Bandettini et al., 1998; Gaab et al., 2007a,b]. Our ROI analysis aims to separate these two effects based on the spatial disparity between the auditory regions and those involved in the default mode, but the influence of the active task on the rest periods and vice versa cannot be fully eliminated in our analysis. One possibility would be to modify the continuous scan by inserting a silent period at the end of the noisy rest period, in order to allow a comparison with the STsamp scan. However, making this period long enough to account for the HRF to decay would unduly lengthen the scan and was considered impractical. Alternatively, using connectivity analyses one could examine spatial relationships of the network.

Additional studies are needed to clarify whether the use of a sparse temporal sampling technique might enhance the diagnostic value that has been proposed for the "default-mode network" [Greicius et al., 2004]. One can argue that the observed differences in the default-mode network between various patient populations [such as Alzheimer's disease, schizophrenia, depression, or attention-deficit hyperactivity disorder; e.g., Greicius et al., 2004, in press; Kennedy et al., 2006; Liang et al., 2006; Lustig et al., 2003; Rombouts et al., 2005; Tian et al., 2006; Wang et al., 2006] and normal controls may be influenced by differences in attention towards SBN.

However, designs that eliminate or reduce SBN during stimuli presentation by reducing the number of acquired

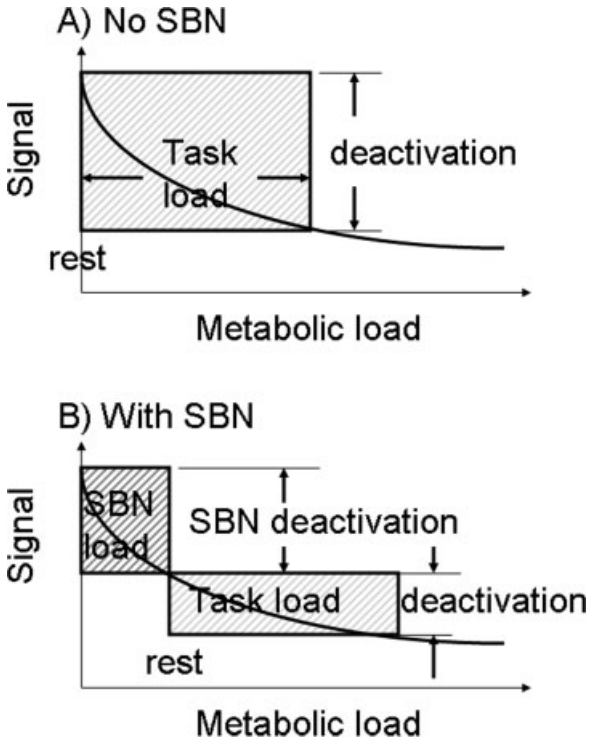

Figure 5.

This figure illustrates the suggested nonlinear influence of SBN on default mode of brain function regions. The abscissa in each part (**A** = SBN absent; **B** = SBN present) represents the amount of work the brain is doing (metabolic load) in default mode of brain function regions. The ordinate represents the signal response. The hypothetical curve shows signal reduction (deactivation) as a nonlinear function of the metabolic load, suggesting a saturation of the deactivation as the total load increases. The blue (light gray/white striped) boxes represent the deactivation within default mode of brain function regions due to the active task. The red box (dark gray/white striped) represents the additional deactivation of SBN being present (increased cognitive or attentional demand). With SBN present, the rest condition shows additional deactivation of the default mode of brain function regions (due to the increased cognitive or attentional demand), which results in a suppression of default mode of brain regions, as confirmed by the results.

images have several other limitations [see Gaab et al., 2007a for an overview]. Therefore, a multifaceted set of variables should be considered prior to the design of an fMRI experiment. Important variables to take in consideration are e.g., subject group, required attention during task, overall difficulty of the task, duration of the experiment, stimulus length, experimental hypothesis, statistical power, or number of conditions [see Gaab et al., 2007a].

CONCLUSION

Research examining the components, characteristics, and purposes of the default-mode network has increased tremendously over the last several years. However, virtually all these studies examined the default-mode network in the presence of SBN, a loud stimulus that has been shown to interfere with attentional demands and task performance.

The present study shows a suppressed default-mode network when assessed in the presence of SBN when compared with the absence of SBN. This finding suggests that (a) resting in "silence" or "noise" may activate a similar network but one that differs in activation magnitudes, and (b) that even passive sensory stimulation leads to decreased activation within default-mode network. Although the term "resting" is often used to describe the condition in which no task is performed and default-mode network activation occurs, such a "resting" condition in fMRI typically occurs in the presence of loud noise. Further studies examining the degree of the influence of SBN on the default-mode network will be needed to clarify and quantify whether the use of a SBN-free sparse temporal sampling technique might enhance the diagnostic value that has been proposed for the "default-mode network".

ACKNOWLEDGMENTS

We thank Allyson Rosen, Alison Adcock, and Arul Thangavel for providing the recorded words. Furthermore, we thank Heesoo Kim for assistance with the analysis.

REFERENCES

Amaro E Jr, Williams SC, Shergill SS, Fu CH, MacSweeney M, Picchioni MM, Brammer MJ, McGuire PK (2002): Acoustic noise and functional magnetic resonance imaging: Current strategies and future prospects. J Magn Reson Imaging 16:497–510.

Bandettini PA, Jesmanowicz A, Van Kylen J, Birn RM, Hyde JS (1998): Functional MRI of brain activation induced by scanner acoustic noise. Magn Reson Med 39:410–416.

Belin P, Zatorre RJ, Hoge R, Evans AC, Pike B (1999): Event-related fMRI of the auditory cortex. Neuroimage 10:417–429.

Binder JR, Frost JA, Hammeke TA, Bellgowan PS, Rao SM, Cox RW (1999): Conceptual processing during the conscious resting state. A functional MRI study. J Cogn Neurosci 11:80–95.

Daselaar SM, Prince SE, Cabeza R (2004): When less means more: Deactivations during encoding that predict subsequent memory. Neuroimage 23:921–927.

Fox MD, Snyder AZ, Vincent JL, Corbetta M, Van Essen DC, Raichle ME (2005): The human brain is intrinsically organized into dynamic, anticorrelated functional networks. Proc Natl Acad Sci USA 102:9673–9678.

Fransson P (2005): Spontaneous low-frequency BOLD signal fluctuations: An fMRI investigation of the resting-state default mode of brain function hypothesis. Hum Brain Mapp 26:15–29.

Friston KJ, Holmes A, Worsley KJ, Poline JB, Frith CD, Frackowiak RSJ (1995): Statistical parametric maps in functional imaging: A general linear approach. Hum Brain Mapp 2:189–210.

Gaab N, Gaser C, Zaehle T, Jancke L, Schlaug G (2003): Functional anatomy of pitch memory--an fMRI study with sparse temporal sampling. Neuroimage 19:1417–1426.

Gaab N, Gabrieli JDE, Glover GH (2007a): Assesing the influence of scanner background noise on auditory processing. I. An fMRI study comparing three experimental designs with varying degrees of scanner noise. Hum Brain Mapp 28: 703–20.

Gaab N, Gabrieli JDE, Glover GH (2007b): Assesing the influence of scanner background noise on auditory processing. II. An fMRI study comparing auditory processing in the absence and presence of recorded scanner noise using a sparse design. Hum Brain Mapp 28:721–32.

Glover GH (1999): Deconvolution of impulse response in event-related BOLD fMRI. Neuroimage 9:416–429.

Glover GH, Law CS (2001): Spiral-in/out BOLD fMRI for increased SNR and reduced susceptibility artifacts. Magn Reson Med 46:515–522.

Greicius MD, Menon V (2004): Default-mode activity during a passive sensory task: Uncoupled from deactivation but impacting activation. J Cogn Neurosci 16:1484–1492.

Greicius MD, Krasnow B, Reiss AL, Menon V (2003): Functional connectivity in the resting brain: A network analysis of the default mode hypothesis. Proc Natl Acad Sci USA 100:253–258.

Greicius MD, Srivastava G, Reiss AL, Menon V (2004): Default-mode network activity distinguishes Alzheimer's disease from healthy aging: Evidence from functional MRI. Proc Natl Acad Sci USA 101:4637–4642.

Greicius MD, Flores BH, Menon V, Glover GH, Solvason HB, Kenna H, Reiss AL, Schatzberg AF (2007): Resting-state functional connectivity in major depression: Abnormally increased contributions from subgenual cingulate cortex and thalamus. Biol Psychiatry 62:429–437.

Gusnard DA (2005): Being a self: Considerations from functional imaging. Consciousness Cogn 14:679–697.

Gusnard DA, Raichle ME (2001): Searching for a baseline: Functional imaging and the resting human brain. Nat Rev Neurosci 2:685–694.

Gusnard DA, Akbudak E, Shulman GL, Raichle ME (2001): Medial prefrontal cortex and self-referential mental activity: Relation to a default mode of brain function. Proc Natl Acad Sci USA 98:4259–4264.

Hall DA, Summerfield AQ, Goncalves MS, Foster JR, Palmer AR, Bowtell RW (2000): Time-course of the auditory BOLD response to scanner noise. Magn Reson Med 43:601–606.

Kennedy DP, Redcay E, Courchesne E (2006): Failing to deactivate: Resting functional abnormalities in autism. Proc Natl Acad Sci USA 103:8275–8280.

Kim DH, Adalsteinsson E, Glover GH, Spielman DM (2002): Regularized higher-order in vivo shimming. Magn Reson Med 48:715–722.

Liang M, Zhou Y, Jiang T, Liu Z, Tian L, Liu H, Hao Y (2006): Widespread functional disconnectivity in schizophrenia with resting-state functional magnetic resonance imaging. Neuroreport 17:209–213.

Lustig C, Snyder AZ, Bhakta M, O'Brien KC, McAvoy M, Raichle ME, Morris JC, Buckner RL (2003): Functional deactivations: Change with age and dementia of the Alzheimer type. Proc Natl Acad Sci USA 100:14504–14509.

Mazoyer B, Zago L, Mellet E, Bricogne S, Etard O, Houde O, Crivello F, Joliot M, Petit L, Tzourio-Mazoyer N (2001): Cortical networks for working memory and executive function sustain the conscious resting state in man. Brain Res Bull 54:287–298.

McKiernan KA, Kaufman JN, Kucera-Thompson J, Binder JR (2003): A parametric manipulation of factors affecting task-induced deactivation in functional neuroimaging. J Cogn Neurosci 15:394–408.

Moelker A, Pattynama PM (2003): Acoustic noise concerns in functional magnetic resonance imaging. Hum Brain Mapp 20:123–141.

Raichle ME, MacLeod AM, Snyder AZ, Powers WJ, Gusnard DA, Shulman GL (2001): A default mode of brain function. Proc Natl Acad Sci USA 98:676–682.

Rombouts SA, Barkhof F, Goekoop R, Stam CJ, Scheltens P (2005): Altered resting state networks in mild cognitive impairment and mild Alzheimer's disease: An fMRI study. Hum Brain Mapp 26:231–239.

Talavage TM, Edmister WB (2004): Nonlinearity of FMRI responses in human auditory cortex. Hum Brain Mapp 22:216–228.

Tian L, Jiang T, Wang Y, Zang Y, He Y, Liang M, Sui M, Cao Q, Hu S, Peng M, Zhuo Y (2006): Altered resting-state functional connectivity patterns of anterior cingulate cortex in adolescents with attention deficit hyperactivity disorder. Neurosci Lett 400:39–43.

Tomasi D, Caparelli EC, Chang L, Ernst T (2005): fMRI-acoustic noise alters brain activation during working memory tasks. Neuroimage 27:377–386.

Wang L, Zang Y, He Y, Liang M, Zhang X, Tian L, Wu T, Jiang T, Li K (2006): Changes in hippocampal connectivity in the early stages of Alzheimer's disease: Evidence from resting state fMRI. Neuroimage 31:496–504.